ISEIS

Journal of Environmental Informatics 18(1) 1-11 (2011)

Journal of Environmental Informatics

www.iseis.org/jei

Parametric Influence on Prediction of Sound Absorption Coefficients for Asphalt Pavements

P. Sachakamol and L. Dai*

Industrial Systems Engineering, Faculty of Engineering and Applied Science, University of Regina, Regina, Saskathewan S4S 0A2, Canada

Received 2 October 2010; revised 27 May 2011; accepted 2 June 2011; published online 12 September 2011

ABSTRACT. A quantitative method for predicting the sound absorption coefficients of various porous highway pavement materials is developed in this research. Types of pavements and material properties of the pavements are considered. Existing models have been evaluated and extended to predict the absorption coefficients of porous materials as a function of their permeability, porosity, and pavement thickness. Experiments are performed on the samples taken from the field and the experimental results are compared with the predicted values of the present method. The effects of several control parameters on the determination of the absorption coefficients are also investigated.

Keywords: sound absorption coefficient, porous materials, pavement, traffic noise, permeability, porosity, tortuosity, sound absorption model

1. Introduction

Research has revealed that tire/pavement noise is a major source of vehicle noise at high velocities (Sandberg and Ejsmont, 2002). Therefore, the use of "quiet pavements" has become an accepted tool for reducing traffic noise at the source, relative to conventional pavement surfaces. In the past few decades, several "quiet pavements", which absorb more sound than conventional pavement due to their structures, have been developed and applied in practice. Two of the most commonly used "quiet pavements" are porous and rubber asphalt pavements due to their advantages in traffic noise reduction.

This research focuses on the prediction of sound absorption coefficients for various pavements and their acoustic parametric influence. Specific attention is paid to a newly developed porous pavement called Asphalt Rubber Concrete (ARC). An article by Gao et al. (2004) and a reference book by Sandberg and Ejsmony (2002) concluded that the noise absorption is the largest contributing factor to noise reduction with porous road pavements. A study conducted by Zhu and Carlson (1999) also confirmed crumb rubber pavement has a stronger ability to absorb sound than some noise barriers in current use, especially within the frequency range of 1 to 5 kHz. These provide a valid argument for making an effort to improve sound absorption therefore reduce traffic noise with porous pavement.

Calculations used for quantifying characteristic quantities of a porous pavement and its predicted sound absorption coefficients depend on the acoustic properties of the pavement material. The materials studied by Delany and Bazley (1970) had porosities near unity and an air path almost unaffected by the presence of the pores which led to the conclusion the that specific airflow resistance is the only physical parameter affectting the sound absorption coefficients. However, their well-known empirical model, which depends primarily on the static airflow resistivity of the porous layer, was only valid at low frequencies. Johnson et al. (1987) introduced several constitutive parameters for predicting the sound absorption coefficient, for example, dynamic permeability and tortuosity.

The micro-structural model proposed by Champoux and Stinson (1992) provided a good physical description for the acoustic properties of porous pavement via five independent parameters used to characterize the material. These were the porosity, airflow resistivity, tortuosity, viscosity and thermal pore shape factor. A theoretical model by Hamet and Berengier (1993) related the same parameters to the macroscopic acoustic absorption coefficient.

Johnson et al. (1987) and Allard and Champoux (1992) provided a similar prediction to the Delany and Bazley model (1970) using the general frequency dependence of viscous forces in porous materials but it was valid at low frequencies. The model by Johnson et al. (1987) and Allard and Champoux (1992) represented the empirical power law predictions in the medium frequency range and also provided a smooth transition to the low frequency region when predicting the correct

* Corresponding author. Tel.: +1 306 5854498; fax: +1 306 5854855.
E-mail address: liming.dai@uregina.ca (L. Dai).

ISSN: 1726-2135 print/1684-8799 online
 doi:10.3808/jei.201100193

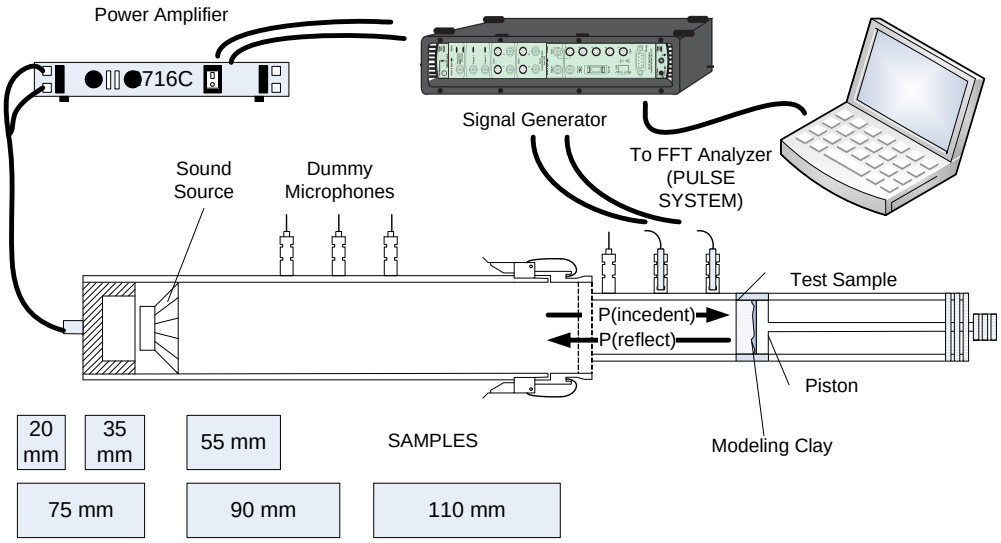

Figure 1. Schematic drawing for the two-microphone method.

limiting behavior of the bulk acoustic properties. The dynamic density and dynamic bulk modulus of porous materials are introduced to solve problems associated with the low frequency range in previous models (Delany and Bazley, 1970).

Table 1. Description of Various Highway Pavement Materials and Test Sections in Saskatchewan

Abbreviation	Description
ARC	Asphalt Rubber Concrete pavement.
AC	Conventional Asphalt Concrete pavement overlay.
New AC	Newer conventional asphalt concrete pavement overlay.
Old AC	Very old and rough conventional asphalt concrete pavement.
New GAS	New pavement with graded aggregate seal.
New CS	New pavement with washed chip seal.
Old CS	Old pavement with washed chip seal.
Flush	Conventional asphalt concrete with a recent flush coat.
RACS	Rubberized asphalt crack seal on newer pavement.
Thermo	Older pavement with a recent thermo patch.

Berengier et al. (1997) developed a theoretical prediction based upon models describing the surface impedance and sound propagation through pavement. A phenomenological and micro-structural approach was combined to account for viscous and thermal effects inside the porous structure.

Sound absorption by porous asphalt pavement is affected by several parameters such as porosity, permeability and the layer thickness (Sachakamol and Dai, 2009). Thus, an optimazed road pavement design can enhance sound absorption by the pavement while maintaining an adequate physical structure (Dai and Lou, 2008; Lou, 2007). Although numerous investigations have been performed on predicting sound absorption by pavement and the effects of porous pavement materials on traffic noise reduction, a reliable and practically sound quantitative methodology is still lacking. An improved model for quantitatively predicting sound absorption coefficients based on fundamental parameters such as porosity, airflow resistivity and tortuosity is to be developed in this research from existing models in the literature. A theoretical absorption coefficient model is to be extended to combine the advantages of phenomenological and micro-structural models. The model is a function of frequency, the surface layer thickness and three physical parameters representative of the porous pavements. This research is also to establish a new algorithm to predict the sound absorption coefficient. The model to be developed is based on experimental tests on specimens taken from the field. The main parameters affecting the sound absorption of porous pavement materials are to be identified and introduced in the quantified model. The numerically simulated results will be compared with experimental data for verification and acoustic analysis.

2. Sound Absorption Coefficient Experimental Setup

The standard used for measuring the acoustic properties of the materials in the present set of experiments, namely the sound absorption coefficients, is ISO 10534-1 (1996). A specific method called the two-microphone, or transfer-function, method for measuring absorption and impedance of acoustic materials is utilized in this research. The equipment and test conditions for the measurements performed in the research exceed the minimum requirements of this standard; ensuring reliable data can be obtained.

The experimental arrangement for the impedance tube tests is shown schematically in Figure 1. The specimens are cut into several sample with a 63.4 mm external diameter; 20, 35, 55, 75, 90 and 110 mm in thickness. Teflon tape was wra-

pped around the external surface of the cylindrical samples to minimize the air gap inside the tube and seal the specimens in the tube with inner diameter of 63.4 mm. A layer of modeling clay is placed between the sample and piston disk, so there is no air gap between them. A test sample of the material is placed in a sample holder and mounted on one end of a straight tube. A rigid plunger with an adjustable depth is placed behind the sample to provide a reflective surface. The tube has a limited frequency range between 100 and 3200 Hz. A Bruel and Kjaer Stereo Audio Power Amplifier 2716C is connected to the opposite end of the tube with a signal generator, Bruel and Kjaer 3560-C-S35, for generating sound. A pair of microphones is mounted flush with the inner wall of the tube near the end of the sample tube. The signal generator is connected with a computer with PULSE 8.0 software for data collection and signal processing.

The specimens were obtained from different pavement surfaces on highways in Regina, Saskatchewan, Canada with the assistance of the Saskatchewan Ministry of Highways and Infrastructure. A description of the sample materials is provided in Table 1. The design and properties of the ARC pavement materials are in the Appendix at the end of this paper. The objectives of the experiment are: 1) to compare different concrete pavements which were paved at the same time, namely Asphalt Rubber Concrete (ARC) and Conventional Asphalt Concrete, in terms of acoustic properties, 2) to compare different surface treatments from various mixtures in terms of their acoustic properties and 3) to study the influence of parametric changes on the acoustic characteristics of various pavement materials that affect their overall sound absorption capabilities.

In the table, the pavements of 5 or more years are considered "old" those pavements of 10 or more years are considered as "very old". The experimental test includes ten pavements, one Asphalt Rubber Concrete and nine different Conventional Asphalt Concrete pavements, all of varying age and surface conditions.

3. Quantitative Model Development

The capability of porous asphalt pavement to absorb sound is affected by several parameters of pavement materials such as the pavement's surface layer thickness, percentage of accessible porosity, pore size and pore aperture size of the material. Thus, an appropriate porous asphalt pavement design can increase noise absorption and, therefore, provide a quiet and comfortable environment for nearby residential areas. To fulfill the requirements of such a design, the quantitative model for pavement noise absorption to be developed in this research intends to assist such design process. This model removes the frequency limitations found in previous models and takes a much wider frequency range into consideration to include the low, medium and high frequency ranges, respectively. Fundamental physical parameters of pavement material such as porosity, airflow resistivity, tortuosity and pavement thickness are also considered in the model development, with the application of some necessary conditions and assumptions.

3.1. Sound Absorption Coefficient Modeling

The wearing course of the pavement considered in this research is made with porous material and it is placed on the upper pavement structure. The absorption coefficient (α) of the porous surface considered in this research can be defined by its Surface Impedance (Z) and Characteristic Impedance (Z_C) as stated by Allard (1994):

$$\alpha = 1 - \left| \frac{Z - Z_c}{Z + Z_c} \right|^2 \tag{1}$$

The surface impedance is expressed as:

$$Z = Z_C \frac{Z_B \coth(-ikL) + Z_C}{Z_B + Z_C \coth(-ikL)} \tag{2}$$

where L is the thickness of the surface layer.

In most cases, especially for a single layer, the porous asphalt is laid on an impervious surface whose acoustic impedance is practically infinite relative to the thick solid base. The surface impedance of the layer can be expressed by assuming Z_R is effectively infinite or can be such that (Berengier et al, 1990):

$$Z = Z_C \coth(-ikL) \tag{3}$$

Consider the complex wave number in a function of angular frequency ω, such as:

$$k(\omega) = \omega \sqrt{\frac{\rho_D(\omega)}{K(\omega)}} \tag{4}$$

The characteristic impedance of a porous material can then be obtained by:

$$Z_C(\omega) = \frac{\sqrt{K(\omega)\rho_D(\omega)}}{\Omega} \tag{5}$$

where Ω is the Porosity of the material.

Both complex wave number and characteristic impedance depend on dynamic bulk modulus $K(\omega)$ and Dynamic density (ρ_D). A theoretical model proposed by Allard and Champoux (1992) is employed and modified to illustrate the propagation of sound through porous materials. Three important parameters, porosity, airflow resistivity and tortuosity are added in this research to this model.

The dynamic density, (ρ_D) accounting for the inertial and viscous coupling effects between the rigid frame and the air in an air-saturated porous material, was proposed by Wang and Torng (2001):

$$\rho_D(\omega) = \rho_0\phi\left[1+\frac{R_S\Omega}{i\phi\rho_0\omega}\sqrt{1+\frac{4i\phi^2\mu\rho_0\omega}{R_S{}^2\Gamma^2\Omega^2}}\right] \tag{6}$$

The dynamic bulk modulus of air in a porous material is written as (Champoux and Allard, 1991):

$$K(\omega) = \gamma P_0\left[\gamma-\frac{\gamma-1}{1+\frac{R_S\Omega}{i\phi\rho_0 N_{\mathrm{Pr}}\omega}\sqrt{1+\frac{4i\phi^2\mu\rho_0 N_{\mathrm{Pr}}\omega}{R_S{}^2\Gamma^2\Omega^2}}}\right] \tag{7}$$

where ρ_0 is the density of the undisturbed fluid, ϕ is the tortuosity, R_S is the Airflow Resistivity, μ is the viscosity of air, γ is the heat ratio, P_0 is the Ambient atmosphere pressure, and N_{Pr} is the Prandtl number. The parameter Γ in the above two equations depends only on the geometry of the rigid frame and is defined by Johnson et al. (1987) and Wang and Tong (2001) as:

$$\Gamma = \sqrt{\frac{8\phi\mu}{\Omega R_S}} \tag{8}$$

Hence, Equations (6) and (7) can be simplified as:

$$\rho_D(\omega) = \rho_0\phi\left[1+\frac{R_S\Omega}{i\phi\rho_0\omega}\sqrt{1+\frac{i\phi\rho_0\omega}{2R_S\Omega}}\right] \tag{9}$$

$$K(\omega) = \gamma P_0\left[\gamma-\frac{\gamma-1}{1+\frac{R_S\Omega}{i\phi\rho_0 N_{\mathrm{Pr}}\omega}\sqrt{1+\frac{i\phi\rho_0 N_{\mathrm{Pr}}\omega}{2R_S\Omega}}}\right] \tag{10}$$

A critical frequency, f_c is introduced in the following form, to improve the convergence of the computation with the model:

$$f_c = \frac{R_S\Omega}{2\pi\phi\rho_0} \tag{11}$$

With the critical frequency, Equations (6) and (7) can be further simplified in the following form:

$$\rho_D(\omega) = \rho_0\phi\left[1+\frac{f_c}{if}\sqrt{1+\frac{if}{2f_c}}\right] \tag{12}$$

$$K(\omega) = \gamma P_0\left[\gamma-\frac{\gamma-1}{1+\frac{f_c}{iN_{\mathrm{Pr}}f}\sqrt{1+\frac{iN_{\mathrm{Pr}}f}{2f_c}}}\right] \tag{13}$$

According to the micro-structural approach developed by Champoux and Stinson (1992), the dynamic density can now be defined as:

$$\rho_D(\omega) = \rho_0\phi\left[1+F(\kappa_D)\frac{f_c}{if}\sqrt{1+\frac{if}{2f_c}}\right] \tag{14}$$

where:

$$F(\kappa_D) = -\frac{1}{4}\frac{\kappa_D\sqrt{i}Y\left(\kappa_D\sqrt{i}\right)}{\frac{1-2Y\left(\kappa_D\sqrt{i}\right)}{\left(\kappa_D\sqrt{i}\right)}} \tag{15}$$

$$Y(\xi) = \frac{J_1(\xi)}{J_0(\xi)} \tag{16}$$

As seen in Equation (16), $Y(\xi)$ is the ratio between the Bessel functions of first and zeroth order. The dimensionless parameter, κ_D in Equation (15) can be obtained by using the model from Delany and Bazley (1970):

$$\kappa_D = c_D\sqrt{\frac{8\phi\rho_0\omega}{R_S\Omega}} \tag{17}$$

The thermal dependence is accounted by the dynamic bulk modulus in the micro-structural approach. In this approach, the thermal pore shape factor and bulk modulus are connected in a real granular structure with a complex geometry, to the viscosity dependence inside the material. The dynamic bulk modulus can also be expressed as (Champoux and Allard, 1991):

$$K(\omega) = \gamma P_0\left[\gamma-\left(\frac{\gamma-1}{1+\frac{f_c}{iN_{\mathrm{Pr}}f}\sqrt{1+\frac{iN_{\mathrm{Pr}}f}{2f_c}}}\right)\frac{Y(\Lambda_K)}{\Lambda_K}\right]^{-1} \tag{18}$$

where:

$$\Lambda_K = \sqrt{N_{\mathrm{Pr}}}\kappa_K\sqrt{i} \tag{19}$$

$$\kappa_K = c_K\sqrt{\frac{8\phi\rho_0\omega}{R_S\Omega}} \tag{20}$$

The adjustable parameter c_k is the thermal pore shape factor and c_D in Equation (17) is an adjustable parameter reflecting the material of a real granular structure with a complex geometry.

The porosity, airflow resistivity, and tortuosity of the pavement material can be experimentally measured and to be inserted into Equation (11) to calculate for the parameters. The dynamic density is given by Equation (14) and dynamic bulk modulus from Equation (18). The two calculated parameters can then be placed in Equations (3) and (5) to compute the material's surface and characteristic impedances, respectively. With these parameters determined, the sound absorption coefficient can be finally determined by implementing Equation (1).

This approach assures the consideration of the parameters such as porosity, permeability, airflow resistivity and tortuosity in quantitatively evaluating the sound absorption coefficient, in addition to the regular parameters of pavement materials.

3.2. Experimental Parameters

As indicated in the previous section, porosity, permeability, and tortuosity are material properties of pavement and can be determined experimentally. Application of the established sound absorption prediction model requires additional basic acoustic and physical information as indicated in the model. In this research, porosity Ω and air flow resistivity R_S are measured directly from tests on the samples collected from the field while the tortuosity ϕ is obtained indirectly from the absorption measurement and optimization technique. Core samples of 63.4 mm in diameter and various thickness, 20, 35, 55, 75, 90 and 110 mm, respectively are extracted from actual pavements. Two set of these specimens in specific diameter and thickness are prepared for this research. One of these is used for measuring porosity and permeability; another is used in the impedance tube to determine the sound absorption coefficient.

Porosity is a measure of the void spaces in a material and is measured as a percentage of voids with respect to the overall volume. The porosity of the samples is calculated from experimental data obtained by following the procedure outlined in ASTM D7063-05 (2005). The density of a given sample is calculated using a water displacement method, where the specimen is initially vacuum sealed inside a plastic bag. The plastic bag is cut open, and since the specimen is under vacuum and the air voids are evacuated, water rushed into all the water accessible air voids in the specimen. Then an apparent maximum density can be calculated from the saturated weight of specimen. The fraction of the total number of voids that are accessible to water, the effective fractional porosity, can be calculated from the difference between the apparent maximum density and the dry density of the specimen.

The permeability used for the calculations is measured with a Pressure Decay Profile Permeameter using a pressure decay system. The system is accurate, repeatable and can be much more efficiently operated in comparing with that using a conventional steady state "mini permeameter" (Lee and Dai, 2009). The permeability k_p is calculated from:

$$k_P = \frac{Q\Delta L}{A\Delta h} \tag{21}$$

where the volumetric flow rate, Q of the liquid through a specimen of porous material is proportional to the hydrostatic pressure difference, Δh across the specimen, inversely proportional to change of the thickness, ΔL of the specimen and proportional to the cross sectional area, A. A pressure difference is created between the two faces of a layer of thickness, L creating a steady volume flow rate of fluid per unit area through the sample, Q / A. The airflow resistivity can be calculated from:

$$R_S = \frac{A}{Q}\frac{\Delta h}{L} \tag{22}$$

The relationship between the permeability and airflow resistivity can be established by combining Equations (21) and (22):

$$R_S = \frac{1}{k_P} \tag{23}$$

The unit used for airflow resistivity is MKS Ralys/m where 1 MKS Rayls is equivalent to $1\,Pa \cdot S \cdot m^{-1}$. The unit for permeability obtained from experiment is Darcy, where 1 Darcy is equal to 1 CGS Rayls or 10 MKS Rayls.

The tortuosity used in the calculation can be determined as the integral of the squared derivative of a curve, divided by the length of the curve (Patasius et al, 2005). The tortuosity can range from one to ten using a regression technique to fit the absorption curve of different pavements and thicknesses:

$$\phi = \frac{\int_{f_1}^{f_2} \left(G(f)\right)^2 df}{L} \tag{24}$$

where $G(f)$ is a non-linear regression equation obtained from optimization technique respected to frequency f from different type of pavements with various thickness.

Under standard conditions, air can be considered an ideal gas. A diatomic molecule has three translational and two rotational degrees of freedom. This results in a specific heat ratio (γ) equal to 1.403. The Prandtl number in this research approximates the ratio of the momentum diffusivity to the thermal diffusivity and is estimated to be 0.702 (William, 1994).

The absorption of acoustic energy into the porous material is caused by the dissipation of the fluid's energy through frictional forces existing between the air and pavement pores. Once the sound wave enters the porous material and the sound energy dissipates due to friction, the flow direction of the

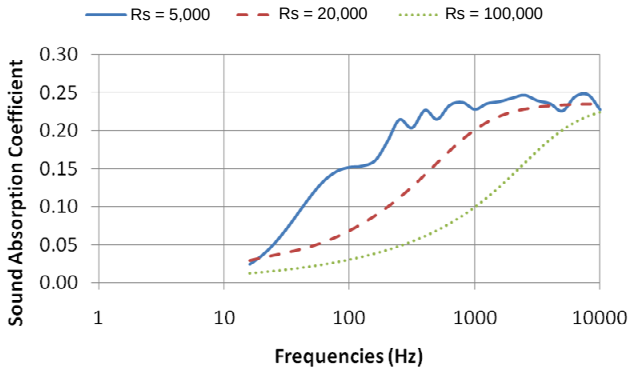

Figure 2. Influence of Specific Airflow Resistance on absorption coefficient, Rs = 5,000, 20,000 and 50,000 MKS Rayls/m, tortuosity = 5, Porosity = 0.15 and thickness = 45 mm.

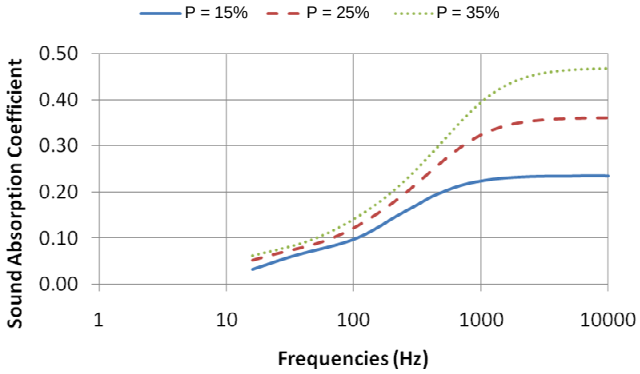

Figure 3. Influence of Porosity on absorption coefficient, P = 15, 25, 35%, tortuosity = 5, Rs = 10,000 MKS Rayls/m and thickness = 45 mm.

sound waves will change. Also, the air molecules will oscillate within the interstices of the porous material at the frequency of the exciting wave whereas the pores undergo periodic compressions and relaxations. The compressions and relaxations determine the absorption capabilities of the pavement materials and depend on the void spaces in a material (porosity), the volume of air passing through (air flow resistivity) and the degree to which the pore is twisted (tortuosity).

4. Parametric Influence

With the availability of the model established, the sound absorption coefficient can be easily determined with all the parameters considered above, and the effects of the parameters on the value of the sound absorption coefficient can be efficiently studied. The value of the controlled parameters are set as, Airflow resistivity equal to 10,000 MKS Rayls/m, Porosity is equal to 15%, Tortuosity is equal to 4.5, and the thickness of pavement is 45 mm. Different values of the parameters under study are applied to the model to predict the Sound Absorption Coefficient for different types of pavements under investigation.

4.1. Effect of Airflow Resistivity

Delany and Bazley (1970) experimentally determined the single physical parameter necessary for a sound absorption prediction model is the specific air flow resistance. The effect of airflow resistivity on the sound absorption coefficient can be quantified with the established model as shown in section 3. For most of the test materials used in this research, the specific airflow resistance has almost no influence on the maximum values of absorption coefficient and its influence become less important at high frequencies. The effect of airflow resistivity on sound absorption coefficient is plotted in Figure 2. The sound absorption coefficient is found inversely proportional to airflow resistivity between 10 and 3,000 Hz. The theoretical explanation for this phenomenon is that it is easier for a shorter wavelength, at higher frequencies, to travel through porous pavement material with a lower airflow resistivity.

4.2. Effect of Porosity

The effect of porosity on the sound absorption coefficient may also be analyzed with the established model. Porosity is a relatively important factor which prominently influences the sound absorption characteristics of porous materials and the maximum values of the sound absorption coefficient. One may notice, as shown in Figure 3, an increase in porosity will increase the maximum level of absorption, as represented by three curves corresponding to P = 0.15, 0.25 and 0.35, respectively. As can be seen from the figure, sound absorption increases as the increase of porosity. It can also be observed that the increase of sound absorption is more significant when frequency becomes large. However, the increase rate of the sound absorption is smaller when frequency is greater than 1000 Hz and the curves tend to be flattened.

4.3. Effect of Tortuosity

The numerical estimates in Figure 4 show the influence of tortuosity on the absorption curve based on the model established. As can be seen from the figure, tortuosity has an influence on the peaks of the sound absorption curve. An increase

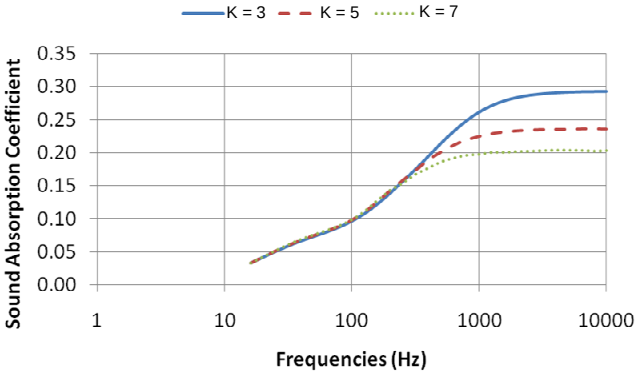

Figure 4. Influence of tortuosity on absorption coefficient, K = 3,5,7 Porosity = 0.15, Rs = 10,000 MKS Rayls/m and thickness = 45 mm.

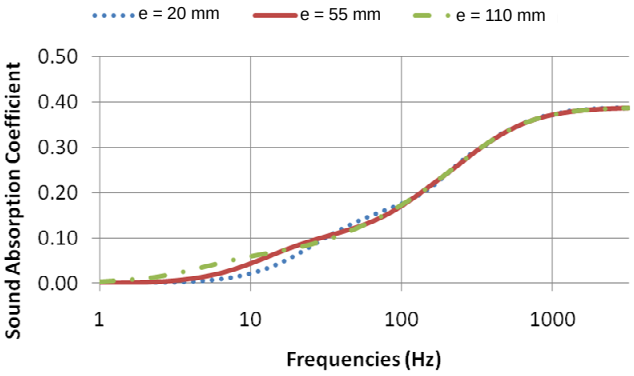

Figure 5. Influence of thickness on absorption coefficient, thickness = 20, 55, 110 mm, tortuosity = 5, Porosity = 0.15, and Rs = 10,000 MKS Rayls/m.

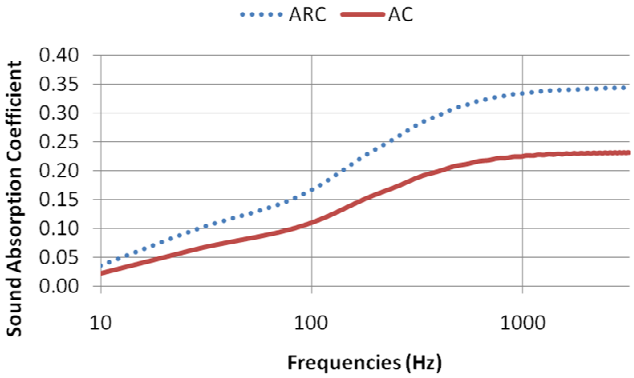

Figure 6. Comparison between measured data of ARC pavement (P = 12.86%, Rs = 2801 MKS Rayls/m, K = 4.0, e = 55 mm) and AC pavement (P = 8.07% Rs = 4310 MKS Rayls/m, K = 4.5, e = 55 mm).

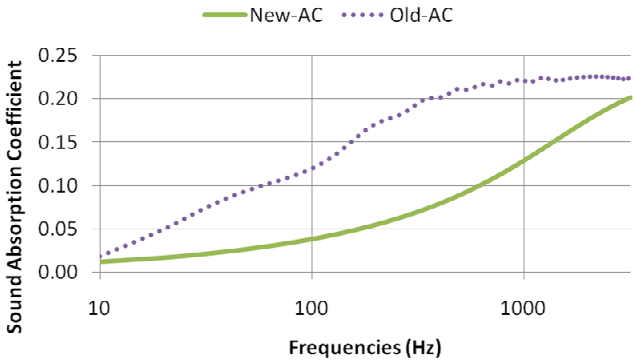

Figure 7. Comparison between measured data of new AC Pavement (P = 8.06%, Rs = 33,333 MKS Rayls/m, K = 4.7, e = 55 mm) and old AC pavement (P = 7.78%, Rs = 3,508 MKS Rayls/m, K = 4.1, e = 55 mm).

in tortuosity decreases maximum sound absorption coefficient. Porosity has the opposite effect, but airflow resistivity has the same effect on the sound absorption curve with tortuosity. Higher tortuosity corresponds to significantly lower sound absorption coefficients as shown in the figure. This implies that the more sound energy is reflected, the less sound is found to traveling in the pores. Low levels of tortuosity have a significant effect on sound absorption for frequencies above 500 Hz. The sound absorption curve does not vary as much at low frequencies.

4.4. Effect of Thickness

The thickness of the porous pavement has a minor effect on the shape and contour of the absorption curve. Figures 5 is plotted to show the absorption curve plateaus at certain lengths as a function of pavement thickness. A thin layer will produce an irresolute curve due to an unstable reflection coefficient and a deficient pavement length for the signal to travel downward and bounce back.

5. Results and Discussion

Experimental measurements are carried out with different test specimens to verify the theoretical model. Their absorption coefficients are measured using two microphones and a standing wave tube method, as shown in Figure 1. The intrinsic characteristics are measured for all ten pavement materials listed in Table 1. Air flow resistivities are measured in accordance with the ISO 10534-1 standard, as well as the porosity and tortuosity of the samples.

Figure 6 shows a comparison between the experimentally measured absorption coefficients of Conventional Asphalt Concrete (AC) pavement which was paved about the same time as the Asphalt Rubber Concrete (ARC) pavement. The peak of the absorption curve from the ARC pavement is in the range of 0.3 to 0.35 whereas the AC pavement is only 0.2 ~ 0.23. Also, the higher absorption coefficient can be seen in the ARC's curve in the low and mid frequency range. It is generally steadier at higher frequencies compared with AC pavement. This may explain why ARC pavement material can reduce traffic noise to a greater extent than AC pavement (Sachakamol and Dai, 2007a, b).

Figure 7 compares the newly paved and 20 year old AC roads where samples are extracted. Results show large differences between the sound absorption coefficient values, especially at mid-range frequencies. The differences are less significant at higher frequencies. Therefore, it can be concluded the pavement's age has a small effect on the peak sound absorption coefficient values in comparison with the other factors. However, the shapes of the sound absorption coefficient curves differ. The older AC pavement possessed relatively higher absorption coefficients. This may be due to the cracks (voids) generated during the period of operation (Patching, 2007) and (Treleaven et al., 2006).

Noise Reduction Coefficient (NRC) values are determined in this research to better represent the comparison between absorption coefficients obtained from numerical simulations and experiments. The NRC is a standard laboratory tested value for determining a sample's ability to absorb sound energy. The higher the NRC value is, the stronger is the sound absorption capabilities of the material. To understand how the

material performs against high, medium and low pitched sound sources, four frequencies at intervals of 250, 500, 1000, and 2000 Hz are required. In particular, the average sound absorption coefficients for a particular surface are calculated at the four frequencies. The experimental test results for the ten materials are listed in Figure 8. ARC obviously displays the highest absorption coefficient which is almost double the value obtained from every other sample. This is in agreement with the field tests where ARC pavement achieved the highest traffic noise reduction relative to the other pavements (Sachakamol and Dai, 2007). Other types of pavement illustrate about the same level of sound absorption and a similar trend in their sound absorption coefficient curves with respected to frequencies.

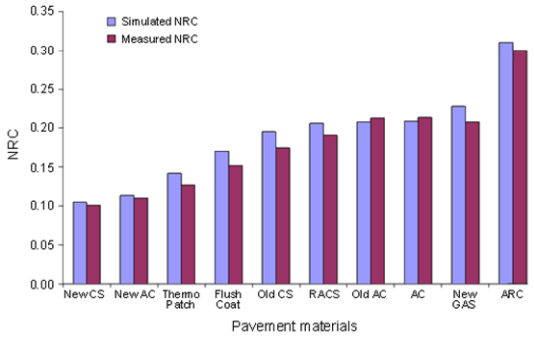

Figure 8. Comparison between NRC values of simulated and measured data.

5.1. Statistical Analysis

Numerical errors are presented in the predicted results from the established model and must be taken into account when comparing them with the data obtained from the experimental procedures. These include truncation errors, created when approximations are used to represent exact mathematical procedures from parametric variables (for example, tortuosity), and round-off errors which occur when data are recorded from experimental measurements. The relationship between the experimental results (from measurements) and approximated results (numerical calculations from the established model) can be formulated as a percent relative error such that:

$$\varepsilon_t = \frac{\text{True error}}{\text{Experimental value}} \times 100\% \tag{25}$$

Let (X_n, Y_n) denote samples of bivariate data from numerical and experimental results, the maximum-likelihood estimator can be obtained with the sample correlation coefficient:

$$R_{SQ} = \frac{\sum_{i=1}^{n}\left(X_i - \bar{X}\right)\left(Y_i - \bar{Y}\right)}{\sqrt{\sum_{i=1}^{n}\left(X_i - \bar{X}\right)^2 \sum_{i=1}^{n}\left(Y_i - \bar{Y}\right)^2}} \tag{26}$$

where $X_i, \bar{X}, Y_i \text{ and } \bar{Y}$ represent the results from predicted samples, the mean of the predicted samples, the experimental measurement samples, and the mean of the experimental measurement samples, respectively. The square of the correlation coefficient is the proportion of variability in a data set that is accounted for by a statistical model, R^2_{SO}. Table 2 shows the predicted and experimental NRC values, including the percent relative error and Coefficient of Determination for various pavements.

Table 2. Comparison between Numerical Errors for Different Samples

	P-NRC*	E-NRC	PRE (%)	Pearson R-Square
ARC	0.31	0.30	2.41	0.96
AC	0.21	0.21	7.08	0.94
New AC	0.11	0.11	4.39	0.96
Old AC	0.21	0.21	5.12	0.93
New GAS	0.23	0.21	5.06	0.94
New CS	0.11	0.10	1.14	0.96
Old CS	0.20	0.17	4.97	0.95
RACS	0.21	0.19	2.26	0.96
Thermo Patch	0.14	0.13	7.90	0.93
Flush Coat	0.17	0.15	5.96	0.95

*P-NRC: Predicted NRC; E-NRC: Experimental measured NRC; PRE: Percentile Relative Error.

The theoretically predictions in Figure 9 show that the line of best fit for the prediction model agrees with the experimental data. The trend line of the frequency dependent absorption coefficient is predicted by comparing the 8,000 simulated values with 8,000 experimental data. The outcome from the statistical analysis indicates the predicted results contain reasonably small errors. In other words, deviations from the predicted values are small. The results indicate a very significant relationship and close agreement between the measured (independent) and predicted (dependent) sound absorption coefficient in the model. Only a small number of predicted data

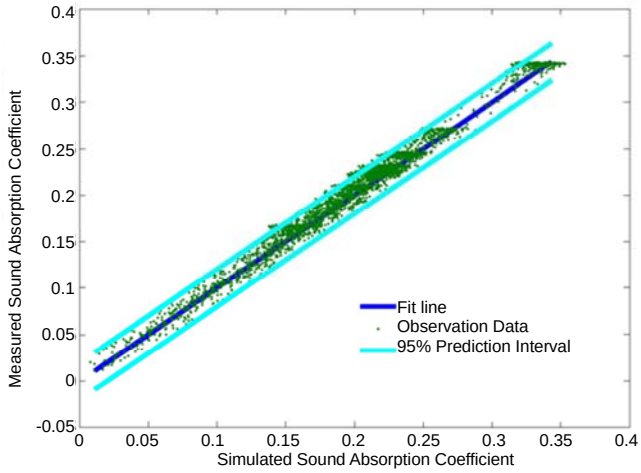

Figure 9. Goodness of fit at 95% Confidence Interval.

exceed the confidence interval at the 95% interval.

The Chi-Square test technique, which is a non-parametric test of statistical significance for bivariate tabular analysis, is used in this research to test the model for goodness-of-fit. Any appropriate test of statistical significance shows the degree of confidence in accepting or rejecting a hypothesis. The hypothesis being tested is the existence of the similarity between the experimental results and predicted data for certain characteristics of the model. Statistically, the non-parametric test like Chi-Square is a rough estimate of the level of confidence (Ott, 1988). It allows data that is less accurate than required for other parametric tests such as t-tests and analysis of variance. Given the overall data set of 8,000 observations, 8,000 data of predicted and experimentally measured noise levels are used in the analysis. The results of the Chi-Square test are shown in Table 3.

This analysis intends to test the hypothesis that the distribution of predicted and experimentally measured data are similar, which will result in the noise prediction model being acceptably accurate. Chi-Square can be calculated by:

$$\chi^2 = \sum_{i=1}^{k} \frac{\left[n_i - np_i\right]^2}{np_i} \tag{27}$$

where k is the number of degrees of freedom, n is the number of samples counted and np_i are the expected values.

Based on the statistical hypothesis and values presented in Table 3, theoretically, it is reasonable to assume the predicted and experimentally measured sound absorption coefficients are normally distributed in a similar fashion. The null hypothesis will be rejected when χ^2 is large. However, due to a very small observed value for χ^2, there is no evidence to reject the null hypothesis. Hence, it can be concluded the two distributions of the predicted and experimentally measured results are the same or similar in their characteristics.

Table 3. Chi-Square Test Results of the Model

Statistical values	Measured α	Predicted α
Mean	0.14	0.16
Known variance	0.00298	0.00297
Observations	8000	8000
Level of significance (α)	0.005	
Degree of freedom	7999	
Chi-Square	163.74	
Null Hypothesis	Failed to reject	

6. Conclusions

An innovative approach for quantitatively evaluating the absorption coefficients of road pavement consisting of porous materials is developed in this research. Various acoustic and physical parameters of the pavement materials, such as porosity, permeability, airflow resistance, tortuosity, pavement thickness, etc, are taken into consideration in the establishment of an analytical model for predicting the effects of porous pavement materials on sound absorption. The parameters under consideration are practically sound and selected so the parameters used in the model established can be conveniently obtained or experimentally determined. The parameters are of primary importance for estimating the sound absorption effects of porous pavement on traffic noise. The developed approach shows reliability and provides accurate results when determining the sound absorption coefficients of porous pavements, in comparison with current approaches. A quantitative approach such as this is not seen in the current literature.

It can be concluded the porosity of the pavement material has a significant effect on sound absorption. This agrees with the conclusions available in the archived documents. Therefore, porosity should be considered when assessing traffic noise reduction over road pavement with porous material. This is significant when considering more porous pavement materials such Asphalt Rubber Concrete (ARC) are increasingly used for road pavement. The advantages of porous pavements on traffic noise reduction are evident, though the mechanism of noise reduction has not been theoretically and completely defined. Among all the pavement materials considered in this research, the rubber mixture pavement material with the highest porosity exhibits the best sound absorption overall.

In terms of the materials parameters, the following can also be concluded from the results:

Airflow resistance, and permeability, of the pavement material tends to affect the shape and size of the absorption curve.

Tortuosity of the pavement material has the opposite effect of porosity on the absorption curve.

The layer thickness of the porous pavement material has an insignificant effect on the sound absorption coefficient in comparison with the other factors concerned. This agrees with the conclusion of Berengier et al (1990).

The results of the established sound absorption coefficient prediction model matches the coefficients experimentally measured using the Two-Microphone method within experimental error. The predicted results show that the established prediction model provides reliable and accurate results with a high level of statistical satisfaction. The goodness of fit between the predicted results from the model and the measured experimental data is also acceptable as per the statistical Chi-Square tests.

The methodology and findings provide practically sound guidance for researchers and engineers to quantitatively predict the sound absorption for porous pavement materials with given material properties. Moreover, the approach contributes to "quite road" design with desired sound absorption levels, material properties and optimal material mixtures.

Acknowledgments. The authors gratefully acknowledge the support from Saskatchewan Highways and Transportation, Communities of Tomorrow (CT), Natural Sciences and Engineering Research Council of Canada (NSERC), and Canada Foundation for Innovation (CFI) for their support of this research.

Appendix

Table A1. Marshall Design

Mix Design Type	Rubber (75Blows)				Mix Design#		C	
Type of Asphalt added	200-300A Binder							
				AGGREGATE GRADATION				
				Stockpile Average % Passing				
	Crushed		Natural	Reclaimed	filler	Hydrated	Design	Spec, Limits
Commodity	Coarse	Fine	Fines	Aggregate	Blender	Lime	Mix	
Proportion	70	30					100.0	
CDN Metric Sieve Series								
18 mm	100	100					100	
16 mm	100	100					100	
12.5 mm	96.9	100					97.8	
9 mm	53.8	99.9					67.6	
5 mm	4.3	86.9					29.1	± 5.0
2 mm	2	48.3					15.9	± 4.0
900 µm	1.7	31.7					10.7	± 3.0
400 µm	1.5	20.4					7.2	± 3.0
160 µm	1.3	12.1					4.5	± 2.0
71 µm	1	8					3.1	± 1.5
% Fracture	97.5	100					97.8	Min 95.0
Sand Equivalent							71.1	Min 45.0
% Light Weight Pieces							0	Max 1.0%
Flat and Elongated							2.3	
Fine Aggregate Angularity							49.7	
% Iron Stone							0.4	
Plasticity Index							NP	

Table A2. Marshall Properties

	Test results		Desirable	Max. Theoretical Specific Gravity	
Property	50 Blow	75 Blow	Results	% Asphalt	T.S.G.
Density		2362		7	2.485
% Air Voids		4.3	3.5% - 4.5%	7.1	2.482
% V.M.A.		18.5	16.0 - 21.0%	7.2	2.479
% V.F.		78.9	68.0 - 83.0%	7.3	2.476
Stability		10878	Minimum 7000n	7.4	2.472
Flow		3.69	2.0mm - 5.0mm	7.6	2.466
Film Thickness		21.87	Minimum 15µm	7.7	2.463
% Retained Stability		100	Minimum 70.0%	7.8	2.46
% Asphalt Absorbed		0.74		7.9	2.457
Dust Proportion Ratio		0.5		8	2.454
Bulk Spec. Grav. Aggregate		2.705	Rice Correction		0.04
DESIGN ASPHALT CONTENT		7.5	Max Specific Gravity		2.469
Asphalt Content of Reclaim			New Asphalt Added to Mix		7.5
% Stripping Potential	0%	Product	None	Retained Tensile Strength	5352/6012 = 89.0%
Mixing Temperature	163c		Compaction Temperature	163c	
COMMENT	Binder includes 20.5% rubber crumb by weight of 200 - 300 Moose Jaw Asphalt;				
	S.G of Liquid Binder is 1.047; Water Absorption is 0.19%				
FORMULA:	% Air Voids= 100[1 - BSGM / TSG]				
	% VOIDS IN MINERAL AGGREGATE (VMA) = 100{1 - (BSGM / (1 + ((ASP / 100) * BSG)}				
	% VOIDS FILLED= ((VMA - AIR VOIDS) / VMA) * 100				
DEFINITIONS:	ASP = Asphalt content in percent by weight of dry aggregate				
	B.S.G = Bulk specific gravity of aggregate				
	B.S.G.M = Bulk specific gravity of compacted mix				
	T.S.G = Theoretical maximum specific gravity corresponding to asphalt content				

References

Allard, J. (1994). Propagation of sound in porous media: modeling sound absorbing material, *J. Acoustiacal Soc. Am.*, 95 (5), 2785-2785. http://dx.doi.org/10.1121/1.409801

Allard, J., and Champoux, Y. (1992). New empirical equations for sound propagation in rigid frame fibrous material, *J. Acoustiacal Soc. Am.*, 91 (6), 3346-3353. http://dx.doi.org/10.1121/1.402824

ASTM D 7063-05 (2005). Standard Test Method for Effective Porosity and Effective Air Voids of Compacted Bituminous Paving Mixture Samples. American Society for Testing and Materials International.

Berengier, M., Stinson, M., Daigle, G., and Hamet, J. (1997). Porous road pavements: Acoustical characterization and propagation effects, *J. Acoustiacal Soc. Am.,* 101 (1), 155-162. http://dx.doi.org/10.1121/1.417998

Berengier, M., Hamet, J., and Bar, P. (1990). Acoustical Properties of Porous Asphalts: Theoretical and Environmental Aspects, *Trans. Res. Record*, 1265.

Champoux, Y., and Allard, J. (1991). Dynamic tortuosity and bulk modulus in air-saturated porous media, *J. Appl. Phys.*, 70 (4), 1975-1979. http://dx.doi.org/10.1063/1.349482

Champoux, Y., and Stinson, M. (1992). On acoustical models for sound propagation in rigid frame porous materials and the influence of shape factors, *J. Acoustiacal Soc. Am.*, 92 (2), 1120-11 31. http://dx.doi.org/10.1121/1.405281

Dai, L. and Lou, Z. (2008). An Experimental and Numerical Study of Tire/Pavement Noise on Porous and Nonporous Pavements, *J. Env. Inform.*, 11(2), 62-73. http://dx.doi.org/10. 3808 /jei.200800112

Delany, M., and Bazley, E. (1970). Acoustical Properties of Fibrous Absorbent Materials, *Appl. Acoustic*, 3 (2), 105-116. http://dx.doi.org/10.1016/0003-682X(70)90031-9

Gao, W., Zhou, H., and Lu, W. (2004). Study on Noise Reduction Properties and Mechanism of Porous Elasitc Road Surface, *Shanghai Environ. Sci.*, 2.

Hamet, J., and Berengier, M. (1993). Acoustical characteristics of porous pavements: A new phenomenological model, *Proceedings of Internoise*, 93, Leuven, Belgium, pp. 641-646.

ISO 10534-1. (1996). Acoustics-Determination of Sound Absorption Coefficient and Impedance in Impedance Tubes-Part 1: Method Using Standing Wave Ration 10534-1, *International Organization for Standardization*.

Johnson, D., Koplik, J., and Dashen, R. (1987). Theory of dynamic permeability and tortuosity in fluid saturated porous media, *J. Fluid Mech.*, 176, 379-402. http://dx.doi.org/10.1017/S002211208 7000727

Lee, H., and Dai, L. (2009). An Experimental and Numerical Approach on Tire/Pavemetn in Counting Pavement Material Characterisitc, *Proceedings of 6th Spring Noise Conference*, Banff.

Lou, Z. (2007). An Experimental and Numerical Study of Tire/Pavement Noise on Asphalt Rubber Concrete Pavement. *MASc Thesis*, University of Regina.

Ott, L. (1988). *An introduction to statistical methods and data analysis (3 ed.)*, PWS-KENT.

Patasius, M., Marozas, V., Lukosevicius, A., and Jegelevicius, D. (2005). Evaluation of tortuosity of eye blood vessels using the integral of square of derivative of curvature, *Proceeding of the 3rd IFMBE European Medical and Biological Engineering Conference (EMBER)*, Prague.

Patching, R. (2007). *Assessment of Rubberized Asphalt ARHM Pavement (Asphalt, Rubberized, Hot Mix) for the Reduction of Traffic Noise*, Patching Associates Acoustical Engineering Ltd.

Sachakamol, P., and Dai, L. (2009). Parametric Inflence on the sound absorption coefficient of porous asphalt, *Proceedings of International Mechanical Engineering Congress and Exhibition*, Lake Buena Vista, Florida.

Sachakamol, P., and Dai, L. (2007a). Road and Tire Noise Emission Assessment with Closed Proximity Method on an Aspalt Rubber Concrete pavement, *Proceedings of Transportation Association of Canada*, Saskatoon, Saskatchewan.

Sachakamol, P., and Dai, L. (2007b). The study of road and tire noise emission from Asphalt Rubber Concrete pavement in Saskatchewan, *Proceedings of CSCE 2007*, Yellowknife, Northwest Territories.

Sandberg, U., and Ejsmont, J. A. (2002). *Tyre/Road Noise Reference Book*, Harg, Kisa, Swenden: INFORMEX Ejsmont and Sandberg Handelsbolag.

Treleaven, L., Pulles, B., Bilawchuk, S., and Donovan, H. (2006). Asphalt Rubber-The Quiet Pavement? *Proceedings of Transportation Association of Canada*, Charlottetown, Prince Edward Island.

Wang, C., and Torng, J. (2001). Experimental study of the absorption characteristics of some porous fibrous materials, *Appl. Acoustics*, 62 (5), 447-459. http://dx.doi.org/10.1016/S0003-682X(00)00043-8

William, M. (1994). Turbulent Prandtl Number-Where Are We? *J. Heat Transfer*, 116 (2), 284-295.

Zhu, H., and Carlson, D. (1999). Asphalt-Rubber: AN Anchor to Crumb Rubber Markets, *Third Joint UNCTAD/IRSG Workshop on Rubber and the Environment, International Rubber Forum*, Veracruz, Mexico.